Driving Force Controller for Electric Vehicle Considering Sideslip Angle Based on Brush Model

Hiroyuki Fuse
The University of Tokyo
5-1-5, Kashiwanoha, Kashiwa, Chiba, 227-8561 Japan
Phone: +81-4-7136-3848
Fax: +81-4-7136-3848
Email: fuse.hiroyuki17@ae.k.u-tokyo.ac.jp

Hiroshi Fujimoto
The University of Tokyo
5-1-5, Kashiwanoha, Kashiwa, Chiba, 227-8561 Japan
Phone: +81-4-7136-4131
Fax: +81-4-7136-4132
Email: fujimoto@k.u-tokyo.ac.jp

***Abstract*—Electric vehicle (EV) has great advantages in vehicle maneuverability with the use of electric motor. As one of EV's motion control methods, a driving force controller with slip ratio limiter has been proposed. In the conventional methods, the value of slip ratio limiter was fixed regardless of sideslip angle of tire. This paper proposes a variable slip ratio limiter considering sideslip angle based on brush model. Driving force controller can secure traction of tire even during cornering. Not only that, it is also suggested that tire workload can be limited to desired value. Its effectiveness was experimentally verified with acceleration cornering on slippery road.**

***Keywords*—Electric Vehicle, vehicle dynamics, maneuverability, driving force controller, brush model, slip ratio control, grip margin**

I. Introduction

Nowadays, electric vehicle (EV) has been a decent candidate for solving environmental problems such as global warming, atmospheric pollution. However, EV has relatively short driving range because of the capacity of the limited energy storage and a lot of research has been done in order to extend the short range [1] [2]. Not only EV shows its environmental potential, it has several advantages in controllability and maneuverability since it is equipped with electric motors [3]. They are

1) Fast torque control response within several milliseconds
2) Torque and driving force can be easily estimated
3) Capability of both driving and regenerating
4) Capability of independent-four-wheel-drive (4WD) system

Using these advantages, a lot of traction control and motion stabilization methods have been proposed [4] [5].

The authors' group has been proposed a driving force controller (DFC) [4]. The DFC controls driving force references while maintaining tire's traction which is realized by limiting slip ratio within certain range. By applying DFC to each wheel, the traction of all wheels can be guaranteed.

Since EV is capable of independent 4WD system, how to distribute each wheel's driving force is important. Driving force distribution methods have been proposed using mainly two ways: the one is based on tire workload [6] [7], and the other is slip ratio. The authors' group has proposed the latter approach [8] [9]. The study [9] proposed a driving force distribution method that minimize maximum slip ratio of all wheels with small calculation cost. Therefore, EV can drive safely on a road which has different friction coefficient on the surface(so called "split-μ road").

However, the previous driving force distribution methods are only applicable for going on straightways since slip ratio limiter is fixed regardless of slip angle of tire. To improve the conventional driving force distribution methods, the author proposed a driving force control method considering slip angle based on "λ–Method" tire model [10]. In the proposed method, the value of slip ratio limiter changes according to slip angle so that tire always keeps its traction even when cornering. However, the proposed method only deals with tire which has equal stiffness on longitudinal and lateral direction.

On the other hand, this study shows a driving force control method considering slip angle based on brush model. It enables us to deal with wider range of tires which have different stiffness on longitudinal and lateral direction. Furthermore, this method also suggests that tire workload can be limited to desired value. Therefore, we can secure certain margin of tire force and thus safe maneuver. The effectiveness of the proposed method is verified by an experiment of acceleration cornering on slippery road.

II. Vehicle Model

A. Vehicle model

In this paper, we consider a vehicle that is capable of independent-4WD. Fig. 1 shows an illustration of the vehicle model.

In the figure, a_x, a_y, V, β, γ, α_{ij}, F_{xij}, F_{yij}, and δ_f are longitudinal, lateral acceleration, vehicle velocity, vehicle's sideslip angle, yaw rate, sideslip angle, longitudinal force, lateral of each wheel, and front steering angle, respectively. The subscription of i will be f or r, indicating front or rear wheel, and j will be l or r, indicating left or right respectively. Equation of rotation of wheel is given by

$$J_{\omega_i}\dot{\omega_{ij}} = T_{ij} - rF_{xij}, \tag{1}$$

where $J_{\omega_{ij}}$, ω_{ij}, T_{ij}, and r are wheel's inertia, angular velocity, torque, and radius of tire,respectively.

978-1-5386-6959-4/19/$31.00 ©2019 IEEE

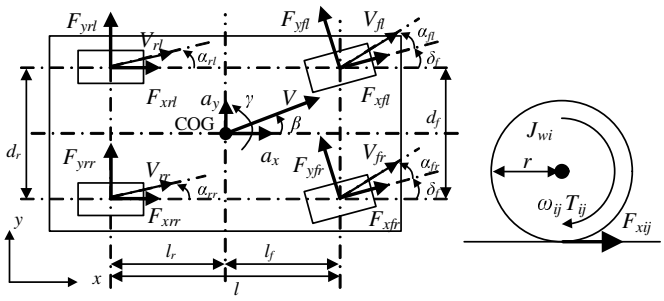

Fig. 1. Vehicle model.

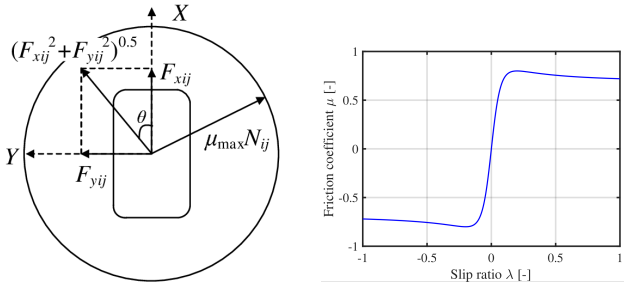

(a) Friction circle. (b) λ–μ curve ($\alpha = 0$).

Fig. 2. Tire force model.

B. Tire Model

To get a better understanding of the DFC and the proposed method later, this section describes basic properties of tire forces and a brush model. It is important to get the exact information of tire forces F_{xij} and F_{yij} so that we can obtain the maneuver of vehicle using the equations of vehicle dynamics above. However, it is not easy to obtain these forces since the generation of tire forces involves complicated friction phenomena between road and tire. Therefore, a lot of tire models have been proposed to emulate the generation of tire forces with different purpose and focus such as brush model [11], Magic Formula [12], and λ-Method tire model [13]. In this paper, we will adopt a brush model.

1) Friction Circle and Tire Workload: Assuming maximum friction coefficient $\mu_{\max}$, resultant force F_{ij}, longitudinal force F_{xij}, lateral force F_{yij}, normal reaction force N_{ij}, and the direction of resultant force θ, the following equations have to be satisfied.

$$F_{ij} = \sqrt{F_{xij}^2 + F_{yij}^2} \leq \mu_{\max} N_{ij} \quad (2)$$

$$\theta = \tan^{-1}(F_{yij}/F_{xij}) \quad (3)$$

This concept is called a friction circle shown in Fig. 2(a), indicating tire force has its limit determined by the condition of road and tire, and normal reaction force acting on tire. Tire workload η_{ij} is defined by

$$\eta_{ij} = \sqrt{F_{xij}^2 + F_{yij}^2}/(\mu_{\max} N_{ij}) \leq 1. \quad (4)$$

2) Generation of Tire Force: In general, longitudinal and lateral force are generated by slip ratio and sideslip angle respectively. In this paper, slip ratio λ_{ij} is defined by

$$\lambda_{ij} = (V_{\omega_{ij}} - V_{ij})/\max(V_{\omega_{ij}}, V_{ij}), \quad (5)$$

where $V_{\omega_{ij}} = r\omega_{ij}$. The relation between slip ratio λ and friction coefficient of road μ is nonlinear as shown in Fig. 2(b). The friction coefficient takes its maximum value $\mu_{\max}$ at a certain slip ratio called optimal slip ratio λ_{p0} when $\alpha = 0$.

3) Brush Model: Brush model assumes countless number of brush-shaped elastic body continuously on the surface of tire. Tire force and its moment are calculated based on the elastic deformation of the brush. a, b, C_x, C_y denote the length and width of contact area, longitudinal and lateral stiffness of the brush, respectively. By assuming that the longitudinal and lateral pressure distributions of contact area are quadratic and constant respectively, resultant force F, longitudinal force F_x, and lateral force F_y of tire are obtained as follows [6].

$$F(\lambda,\alpha) = \begin{cases} \mu_{\max} N s(3 - 3s + s^2), & [0 \leq s \leq 1] \\ \mu_{\max} N, & [s > 1] \end{cases} \quad (6)$$

$$F_x(\lambda,\alpha) = F\cos\theta \quad (7)$$

$$F_y(\lambda,\alpha) = F\sin\theta \quad (8)$$

where s is the normalized length of slipping area divided by a. When $s = 0$, tire is completely adhesive. When $s = 1$, all the contact area becomes slipping area. Since the definition of slip ratio differs in case of acceleration and deceleration, s and θ are respectively represented in each case. In case of acceleration, they are given by

$$\theta(\lambda,\alpha) = -\tan^{-1}\left(\frac{\phi\tan\alpha(1-\lambda)}{\lambda}\right) \quad (9)$$

$$s(\lambda,\alpha) := K\sqrt{\lambda^2 + \phi^2(1-\lambda)^2\tan^2\alpha} \quad (10)$$

$$K := a^2 b C_x/(6\mu_{\max} N), \quad C_y = \phi C_x \quad (11)$$

where K is a parameter determining s and ϕ is a stiffness ratio of longitudinal and lateral direction. On the other hand, in case of deceleration, they are given by

$$\theta(\lambda,\alpha) = -\tan^{-1}\left(\frac{\phi\tan\alpha}{\lambda}\right) \quad (12)$$

$$s(\lambda,\alpha) = K\frac{\sqrt{\lambda^2 + \phi^2\tan^2\alpha}}{1+\lambda} \quad (13)$$

III. Driving Force Controller

In this section, a DFC [8] is explained.

A. Block Diagram and Structure

The block diagram of the DFC is shown in Fig. 3. The outer loop is a driving force loop and the inner loop is a slip ratio/wheel velocity loop that controls the slip ratio. From (1), the driving force of each wheel is estimated by a driving force observer (DFO). F_{xij}^* is the reference longitudinal force and $\hat{F}_{xij}$ is the estimated driving force. The definition of slip ratio has two cases on both acceleration and deceleration. For smoother control, new control input y_{ij} is defined as

$$y_{ij} = (V_{\omega_{ij}} - V_{ij})/V_{ij}. \quad (14)$$

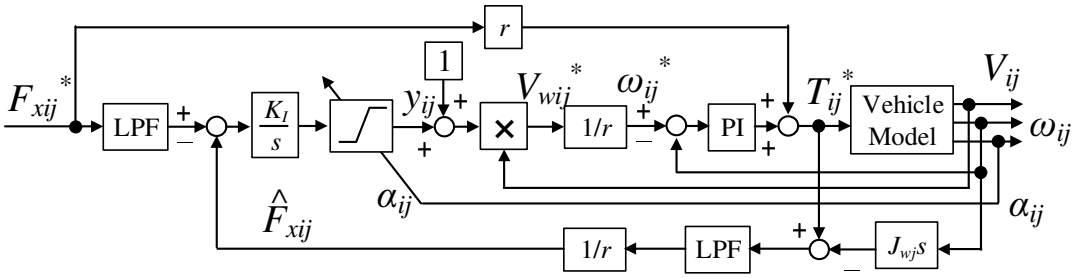

Fig. 3. Driving Force Controller with proposed variable slip ratio limiter.

This is the same definition as that of slip ratio for deceleration. The relationship between y_{ij} and λ_{ij} for acceleration is calculated as

$$y_{ij} = \lambda_{ij}/(1-\lambda_{ij}). \tag{15}$$

y_{ij} approximately equals to λ_{ij} when $|\lambda_{ij}| << 1$ and they are always one to one correspondence. As F^*_{xij} is inputed, feed-forward loop outputs approximately adequate torque reference which ignores the derivative of the angular speed. This secures fast response of the DFC. Inner slip ratio/wheel speed control loop adjusts slight error for precise output. As long as vehicle is on high traction road or F^*_{xij} is not as large as the limit of tire force, DFC operates as a direct torque controller.

B. Slip Ratio Limiter and Traction Control

The equation of tire model (6) suggests that resultant force F is maximized when $s \geq 1$. However, for the controllability of vehicle maneuver and considering the general fact that F rather decreases if tire slips too much [12], $s \leq 1$ is desired. To achieve this, slip ratio's upper and lower limit $y_{ij\max}$ and $y_{ij\min}$ for the integrator of the DFC are added. With this saturation, traction can be retained by keeping the slip ratio within the range where μ is monotonic function of λ (see Fig. 2(b)) if we know certain value of the optimal slip ratio $\lambda_{\rm p0}$, which is easy to estimate using an EV with IWM [14].

IV. Proposed variable slip ratio limit for y

In the previous studies of the DFC [8] [9], the saturation values of $y_{ij\max}$ and $y_{ij\min}$ are fixed in order to limit the slip ratio within $|\lambda| = \lambda_{\rm p0}$. This constant slip ratio limit (or, CSRL) is only effective when vehicle is going straight and there is no sideslip ($\alpha_{ij} = 0$). For example, there will be a situation that intended lateral force cannot be generated when vehicle tries to turn but tire force is already used for longitudinal direction.

To prevent this problem, the author proposed a new method to determine the saturation values according to the change of α_{ij} based on λ-Method tire model [10]. This previous method of variable slip ratio limit (or, VSRL) demonstrated an improvement of controllability and reduction of required steering angle on acceleration cornering.

However, the previous method of VSRL only deals with tire which has equal stiffness on longitudinal and lateral direction. Tire in general has grooves on the surface for the purpose of effective draining so that stiffness can be different with direction. On the other hand, this study proposes a new VSRL based on brush model. This method enable us to handle wider range of tires which have different stiffness on longitudinal and lateral direction.

A. Derivation of Critical Condition ($s = \eta = 1$)

In this paper, "critical condition" means a set of slip ratio λ and sideslip angle α which satisfy $s = 1$ and $\eta = 1$, when tire force is effectively maximized. This section derives the critical condition used for the VSRL of DFC.

1) Derivation of Parameters K and ϕ: K and ϕ are important parameters determining tire forces (see (11)) and needed to be obtained. Here, we assume an optimal slip ratio in case of acceleration $\lambda_{\rm p0t}$ is already known with prior estimation [14]. By the definition of the optimal slip ratio, $\lambda = \lambda_{\rm p0t}$, $\alpha = 0$, and $s = 1$ hold. Therefore, we have a following equation by substituting these conditions to (10).

$$K = 1/\lambda_{\rm p0t} \tag{16}$$

Stiffness ratio ϕ can be obtained by (3) and (9) as follows.

$$\phi = -\frac{F_y \lambda}{F_x \tan\alpha (1-\lambda)} \tag{17}$$

2) Critical Condition for Driving Mode ($\cos\theta > 0$) *:* Combined with (6), (10), and (16), we have the critical condition where $\eta = 1$ and $s = 1$ satisfy for driving mode as follows.

$$\lambda_{\rm p0t} = \sqrt{\lambda^2 + \phi^2 (1-\lambda)^2 \tan^2\alpha} \tag{18}$$

This equation indicates if either of slip ratio λ or sideslip angle α is determined, the other is spontaneously derived.

$$\lambda_{\rm drv}(\alpha) = \frac{\phi^2 \tan^2\alpha + X_1}{1 + \phi^2 \tan^2\alpha} \quad (|\alpha| \leq \alpha_{\max}) \tag{19}$$

$$X_1 := \sqrt{\lambda_{\rm p0t}^2 + (\lambda_{\rm p0t}^2 - 1)\phi^2 \tan^2\alpha} \tag{20}$$

$$\alpha_{\max} := \tan^{-1} \frac{\lambda_{\rm p0t}}{\phi\sqrt{1-\lambda_{\rm p0t}^2}} \tag{21}$$

If we determine value of θ which is the direction of resultant force F, both λ and α can be derived by (9),(18), and (19).

$$\alpha_{\rm drv}(\theta) = -\tan^{-1} \frac{\lambda_{\rm p0t} \sin\theta}{\phi(1 - \lambda_{\rm p0t}\cos\theta)} \tag{22}$$

$$\lambda_{\rm drv}(\theta) = \lambda_{\rm p0t} \cos\theta \tag{23}$$

3) Critical Condition for Braking Mode $(\cos\theta < 0)$ *:* Combined with (6), (13), and (16), we have the critical condition where $\eta = 1$ and $s = 1$ satisfy for braking mode as follows.

$$\lambda_{\mathrm{p0t}} = \frac{\sqrt{\lambda^2 + \phi^2 \tan^2\alpha}}{(1+\lambda)} \tag{24}$$

If we solve (24) for λ, we have

$$\lambda_{\mathrm{brk}}(\alpha) = \frac{\lambda_{\mathrm{p0t}}^2 - X_1}{1 - \lambda_{\mathrm{p0t}}^2} \qquad (|\alpha| \le \alpha_{\max}) \tag{25}$$

If we determine the value of θ, both λ and α can be derived by (12),(24), and (25) as follows.

$$\alpha_{\mathrm{brk}}(\theta) = \alpha_{\mathrm{drv}}(\theta) \tag{26}$$

$$\lambda_{\mathrm{brk}}(\theta) = \frac{\lambda_{\mathrm{p0t}}\cos\theta}{1 - \lambda_{\mathrm{p0t}}\cos\theta} \tag{27}$$

4) VSRL for Critical Condition $(s = 1)$ *:* Tire forces and tire workload are calculated using brush model with the critical conditions of λ and α for $0 \le \theta \le 360$ deg with tire's parameters of $\lambda_{\mathrm{p0t}} = 0.16$, $\phi = 0.8, 1, 1.2$, $\mu_{\max} = 1$, $N = 2500$ N. Three values of the stiffness ratio ϕ were tested to see the difference effectively.

Fig. 4 shows tire force and workload characteristic with the critical condition. Fig. 4(a), Fig. 4(b), Fig. 4(c), and Fig. 4(d) show λ–α characteristic of the critical condition, λ–θ and α–θ characteristics, F–θ and η–θ characteristics, respectively.

For comparison, λ–α characteristic of the critical condition obtained by λ–Method [15] [10] is also shown in Fig. 4(a) and in the following equations (λ–Method assumes $\phi = 1$ in the first place).

$$\lambda_{\mathrm{drv-LM}}(\alpha) = 1 - \frac{1 - \lambda_{\mathrm{p0t}}^2}{\cos\alpha + \sqrt{\cos^2\alpha - 1 + \lambda_{\mathrm{p0t}}^2}} \tag{28}$$

$$\lambda_{\mathrm{brk-LM}}(\alpha) = 1 - \cos\alpha - \sqrt{\cos^2\alpha - 1 + \lambda_{\mathrm{p0t}}^2} \tag{29}$$

It is clearly suggested that the obtained critical conditions of λ and α satisfy $\eta = 1$ for any tire force direction regardless of the change of ϕ. Therefore, (19) and (25) can be used for the VSRL of DFC. Both of the critical condition obtained by brush model in case of $\phi = 1$ (blue line) and λ–Method (black line) have similar curves on right side area (i.e., driving mode). Conversely on the left side area (i.e., braking mode), they are quite different especially where $|\alpha|$ is small. This is because the optimal slip ratio of braking mode λ_{p0b} of both tire models are different while λ_{p0t} are equal, which is easily confirmed by substituting $\alpha = 0$ to (27) and (29).

The slip ratio controller of DFC uses y that is the definition of slip ratio for braking mode. Therefore, the saturation values of $y_{\max}$ and $y_{\min}$ are

$$y_{\max}(\alpha) = \frac{\phi^2 \tan^2\alpha + X_1}{1 - X_1} \tag{30}$$

$$y_{\min}(\alpha) = \frac{\lambda_{\mathrm{p0t}}^2 - X_1}{1 - \lambda_{\mathrm{p0t}}^2} \tag{31}$$

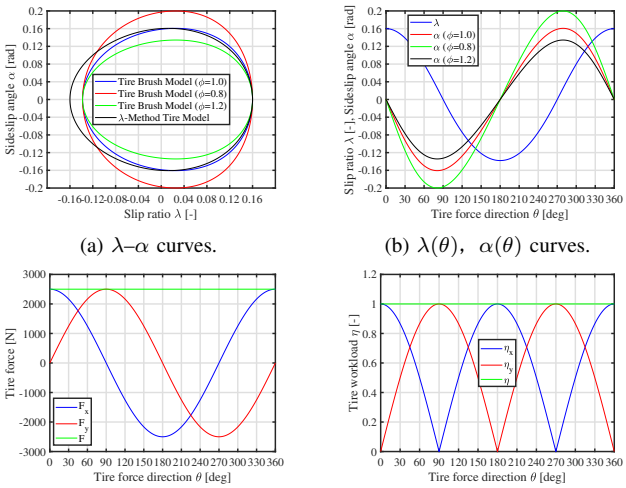

(a) λ–α curves. (b) $\lambda(\theta)$, $\alpha(\theta)$ curves.

(c) $F(\theta)$ curves. (d) $\eta(\theta)$ curves.

Fig. 4. Tire force and workload η with critical condition where $\eta = s = 1$ hold. Regardless of the difference of stiffness ratio ϕ, $\eta = 1$ is successfully maintained.

In case of $|\alpha| \ge \alpha_{\max}$, $s > 1$ holds even if $\lambda = 0$, meaning all the contact area of tire goes slipping. To minimize this, $y_{\max} = y_{\min} = 0$ will be substituted.

B. VSRL with Grip Margin $(s < 1)$

The last section derived the critical condition for the VSRL of DFC. The proposed VSRL can maintain and maximize tire's traction even during cornering. However, unless emergency situation when vehicle needs to maneuver in drastic manner fully using tire's limit, tire's slip should be as low as possible in order to reduce slip power dissipation and extend lifetime of tire. This section suggests a VSRL with certain grip margin of tire for this purpose.

Tire workload η is represented by s from (4) and (6) as follows.

$$\eta = s(3 - 3s + s^2), \quad [0 \le s \le 1] \tag{32}$$

This equation can be solved for s and given by

$$s = 1 - (1 - \eta)^{\frac{1}{3}}, \quad [0 \le \eta \le 1] \tag{33}$$

If we give desired grip margin $m = 1 - \eta$, s_{lim} is derived by

$$s_{\mathrm{lim}} = 1 - m^{\frac{1}{3}}, \quad [0 \le m \le 1] \tag{34}$$

By liming $s \le s_{\mathrm{lim}}$, we can get desired grip margin m. To obtain slip ratio λ and sideslip angle α that satisfy given s_{lim}, $s = s_{\mathrm{lim}}$ should be substituted instead of $s = 1$ to (18) and (24). In other words, all the term λ_{p0t} in the equations of the critical condition should be replaced by $s_{\mathrm{lim}}\lambda_{\mathrm{p0t}}$ instead.

Fig. 5 shows λ, α, and η with desired grip margin $m = 0, 0.1, 0.2$. By reducing magnitude of λ and α compared to the critical condition, calculated η becomes smaller and the desired grip margin is attained.

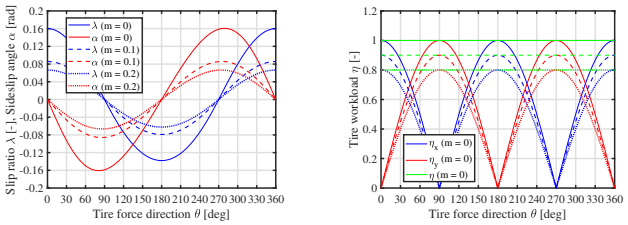

(a) $\lambda(\theta)$, $\alpha(\theta)$ curves. (b) $\eta(\theta)$ curves.

Fig. 5. Slip ratio, sideslip angle, and tire workload with grip margin $m = 0, 0.1, 0.2$.

Fig. 6. Exp. setup.

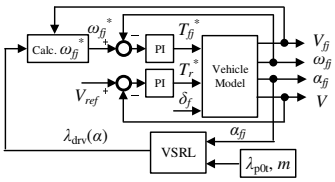

Fig. 7. VSRL controller.

TABLE I
EXPERIMENTAL CONDITION.

λ_{p0t}	ϕ	$\mu_{\max}$	m	V_{ref}
0.16	1.12	0.27	0.3	6 m/s

TABLE II
VEHICLE SPECIFICATION.

Vehicle mass (including driver) M	910 kg
Wheelbase l	1.7 m
Distance from center gravity to front and rear axle l_f,l_r	l_f:1.0 m l_r:0.7 m
Gravity height h_{g}	0.51 m
Front and rear wheel inertia J_{ω_f}, J_{ω_r}	1.24, 1.26 kg·m^2
Wheel radius r	0.302 m

V. EXPERIMENTAL VERIFICATION OF VSRL

We conducted an experiment using a real EV on acceleration cornering on slippery road shown in Fig. 6. The slippery road was emulated by polymer sheets with sprayed water on the surface. To focus on the effect of the VSRL, we used a slip ratio controller with the proposed VSRL shown in Fig. 7. The controller drives front wheels with the slip ratio reference value λ_{p0t}. As driver manually steers wheel and generates tire sideslip angle, the proposed VSRL limits the slip ratio reference to be $\lambda_{\mathrm{drv}}(\alpha)$. Desired tire grip margin m is set to be 0.3. Rear wheels are driven by a vehicle speed controller that maintains constant speed of V_{ref} = 6 m/s. Tab. I shows experimental condition. λ_{p0t}, ϕ, and $\mu_{\max}$ are obtained in advance [14] [16]. It should be noted that the information of $\mu_{\max}$ is only required to estimate tire workload. For comparison, acceleration cornering with the VSRL based on λ–Method (i.e., m is 0) was also carried out.

A. Experimental Vehicle

In this study, we use an EV "FPEV2–Kanon" shown in Fig. 6 for experimental verification. The EV is equipped with a direct-drive in-wheel motor (IWM) in each wheel and capable of independent 4WD control. The equipped IWM has maximum power of 20 kW and speed of 1200 rpm. Tab. II shows the specification of the experimental vehicle.

B. Measurement and Estimation

We use an optimal velocity sensor, acceleration sensor, yaw rate sensor, and wheel speed sensor for obtaining required information of vehicle maneuver. We used an AUTOBOX DS1103 for computation. The sampling rate for the experiment is 20 kHz. Lateral force F_{yij}, sideslip angle α_{ij}, and tire workload η_{ij} were estimated by measured values by the sensors [15]. It should be noted that vehicle velocity V and vehicle's sideslip angle β can be estimated without the use of the optimal velocity sensor which tends to be expensive for commercial vehicles [17], [18], the increase of robustness against measurement deviation and the implementation of the estimation will be future work. .

C. Results

Fig. 8 shows experimental results of the acceleration cornering on slippery road with the VSRL based on λ–Method (m = 0, only front left wheel is shown). Steering angle was increased gradually in this condition. As α_{fl} increases, λ_{fl} decreases from $\lambda_{\mathrm{p0t}} = 0.16$ to zero (Fig. 8(a), Fig. 8(b)). The absolute values of longitudinal force F_{xfl} and lateral force F_{yfl} change in the opposite manner, which shows the effect of the VSRL (Fig. 8(c)). Tire workload η_{fl} is maintained between 0.8 and 1.0 for any tire force direction θ. In this way, tire workload can be maximized thanks to the VSRL.

On the other hand, Fig. 9 shows experimental results with the VSRL based on tire brush model (m = 0.3, only front right wheel is shown). To demonstrate the effectiveness of the proposed method, steering angle was controlled so that sideslip angle changes alternatively. According to the change of α_{fr} λ_{fr} is limited to be much lower than λ_{p0t}, indicating the effect of the VSRL (see Fig. 9(a) and Fig. 9(b)). It is clearly shown in Fig. 9(c) that longitudinal force F_{xfr} conversely increases and decreases compared to the absolute value of lateral force $|F_{yfr}|$. Thanks to the VSRL set to be $m = 0.3$, estimated tire workload η_{fr} was successfully maintained less than 0.7 with the desired grip margin for any tire force direction. Therefore, the proposed VSRL can be applied to conventional DFC so that traction of tire can be maintained. One of reasons that tire workload η_{fr} occasionally exceeds 0.7 is uneven condition of the slippery road.(e.g., gap between sheets).

VI. CONCLUSION

This paper proposed a variable slip ratio limiter for a driving force controller based on brush model. With the proposed method, slip ratio is suppressed while cornering so that enough amount of lateral force can be generated for stable and smoother cornering. Furthermore, it is also suggested that tire workload can be limited to desired value as well. Its effectiveness was verified by an experiment of acceleration cornering on slippery road using a real electric vehicle. In

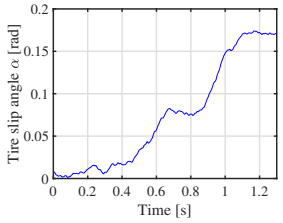

(a) Sideslip angle α_{fl}.

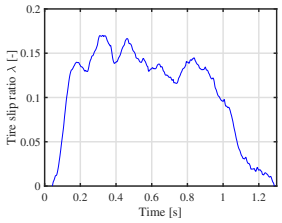

(b) Slip ratio λ_{fl}.

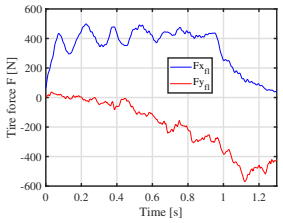

(c) Tire forces F_{xfl}, F_{yfl}.

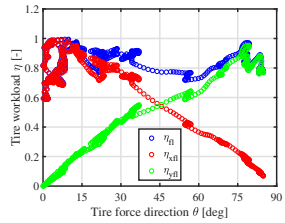

(d) Tire workload η_{fl}.

Fig. 8. Experimental results of acceleration cornering with variable slip ratio limit (m = 0, based on λ–Method).

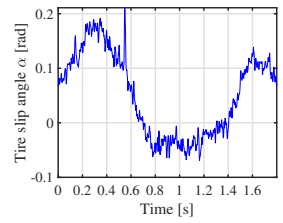

(a) Sideslip angle α_{fr}.

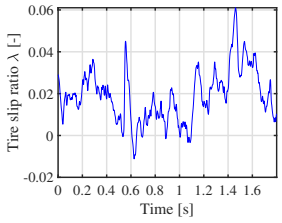

(b) Slip ratio λ_{fr}.

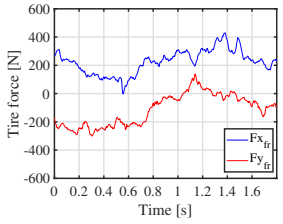

(c) Tire forces F_{xfr}, F_{yfr}.

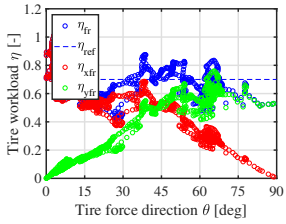

(d) Tire workload η_{fr}.

Fig. 9. Experimental results of acceleration cornering with variable slip ratio limit (m = 0.3). Tire workload was successfully maintained around desired grip margin for any tire force direction.

the experiment, grip margin was set to be 0.3 and estimated tire workload was successfully limited around 0.7. Further experimental verifications on other conditions of grip margin and deceleration mode, and different road condition will be future work.

VII. Acknowledgments

This research was partly supported by Industrial Technology Research Grant Program from New Energy and Industrial Technology Development Organization (NEDO) of Japan (number 05A48701d), the Ministry of Education, Culture, Sports, Science and Technology grant (number 22246057 and 26249061).

References

[1] Y. Ikezawa, et. al., "Range Extension Autonomous Driving for Electric Vehicles Based on Optimal Velocity Trajectory Generation and Front-Rear Driving-Braking Force Distribution," IEEJ J. Industry Applications, vol. 5, no. 3, pp. 228–235, 2016.

[2] G. Lovison, et. al.,"Secondary-side-only Control for High Efficiency and Desired Power with Two Converters in Wireless Power Transfer Systems,"IEEJ J. Industry Applications, vol. 6, no. 6, pp. 473–481, 2017.

[3] Y. Hori, "Future vehicle driven by electricity and control research on four-wheel-motored "UOT electric march II"", IEEE Trans. Industrial Electronics, 51, 5, pp. 954-962 (2004).

[4] M. Yoshimura and H. Fujimoto, "Driving torque control method for electric vehicle with in-wheel motors", IEEJ Transactions on Industry Applications, Vol. 131, No. 5, pp.1-8 (2010) (in Japanese).

[5] M. Kamachi, and K. Walters: "A Research of Direct Yaw- Moment Control on Slippery Road for In-Wheel Motor Vehicle", The 22nd International Battery, Hybrid and Fuel Cell Electric Vehicle Symposium and Exposition, Yokohama, Japan, pp. 2122-2133 (2006).

[6] O. Nishihara, and S. Higashino: "Exact Optimization of Four-Wheel Steering and Four-Wheel Independent Driving/Braking Force Distribution with Minimax Criterion of Tire Workload", Transactions of the Japan Society of Mechanical Engineers C,Vol.79, No.799, pp.629-644, (2013). (in Japanese)

[7] O. Mokhiamar and M. Abe: "Effects of An Optimum Cooperative Chassis Control From The View Points of Tire Workload", Proc. of JSAE 2003 Annual Congress, No. 33-03, pp.15-20 (2003).

[8] K. Maeda, H. Fujimoto, and Y. Hori: "Four-wheel Driving force Distribution Method for Instantaneous or Split Slippery Roads for Electric Vehicle with in-wheel motors", 12th IEEE International Workshop on Advanced Motion Control, pp. 1-6. (2012).

[9] N.Shimoya, H.Fujimoto, "Fundamental Study of Driving Force Distribution Method for Minimization of Maximum Slip Ratio for Electric Vehicles with In-wheel Motors", International Electric Vehicle Technology Conference (EVTeC), 2016.

[10] H. Fuse, H. Fujimoto. "Fundamental Study on Driving Force Control Method for Independent-Four-Wheel-Drive Electric Vehicle Considering Tire Slip Angle", IEEE conference IECON2018, 2018.

[11] O. Nishihara, et-al, "Estimation of Road Friction Coefficient Based on the Brush Model", Transactions of the Japan Society of Mechanical Engineers Series C 75(753), 1516-1524, 2009. (in Japanese).

[12] H. B. Pacejka and E. Bakker, "The Magic Formula Tyre Model," Vehicle System Dynamics: International Journal of Vehicle Mechanics and Mobility, Vol. 21, No. 1, pp. 1-18 (1992).

[13] Y. Horiuchi, "A proposition of the simple tire model for the Vehicle Stability Assist system", Society of Automotive Engineers of Japan, preceding of congress, No.64-98, (1998). (in Japanese)

[14] H. Fuse, et.al. "Minimum-time Maneuver and Friction Coefficient Estimation Using Slip Ratio Control for Autonomously-Driven Electric Vehicle", IEEJ SAMCON2018, 2018.

[15] H. Fuse, H. Fujimoto, "Effective Tire Force Vector Control and Maximization Method for Independent-Four-Wheel-Drive Electric Vehicle, The 2018 IEEE International Transportation Electrification Conference & EXPO Asia-Pacific", Bangkok, Thailand, Session 8A2-2, Proceedings pp.54 (2018).

[16] K. Maeda, H. Fujimoto, Y. Hori, "Driving Force Control of Electric Vehicle Based on Optimal Slip Ratio Estimation Using brush model", JIASC, Vol. IV, pp. 137-140, 2012.

[17] K. Fujii, H. Fujimoto, "Traction Control based on Slip Ratio Estimation Without Detecting Vehicle Speed for Electric Vehicle", IEEE, Power Conversion Conference, 2007.

[18] C. Geng, T. Uchida, Y. Hori, "Body Slip Angle Estimation and Control for Electric Vehicle with In-Wheel Motors", IEEE conference IECON 2007.